Ceramics International xxx (xxxx) xxx

Contents lists available at ScienceDirect

Ceramics International

journal homepage: www.elsevier.com/locate/ceramint

Effects of zirconia additives on β-tricalcium-phosphate cement for high strength and high injectability

Yeeun Kim [a], Jiyoung Bae [a,1], Emi Uyama [a], Kazumitsu Sekine [a], Fumiaki Kawano [b], Kenichi Hamada [a,*]

[a] Department of Biomaterials and Bioengineering, Tokushima University Graduate School of Biomedical Sciences, 3-18-15 Kuramoto, Tokushima 770-8504, Japan
[b] Department of Comprehensive Dentistry, Tokushima University Graduate School of Biomedical Sciences, 3-18-15 Kuramoto, Tokushima 770-8504, Japan

ARTICLE INFO

Keywords:
Zirconia additives
Calcium phosphate cement
Mechanical properties
Injectability

ABSTRACT

Injectable calcium phosphate cements (CPCs) exhibit many advantages as bone substitution materials. However, the strength of injectable CPCs after setting are often insufficient. In our previous studies, mechano-chemically modification of β-tricalcium phosphate cement powder through a planetary ball-milling process exhibited simultaneous improvement in the strength and injectability of CPC. Two plausible effects of this process are: changes in the CPC powder properties and zirconia abrasion powder contamination from the milling pot and balls. The objective of the present study is to separately evaluate these two effects on the strength and injectability of CPCs.

The calculated injectability of the cement paste with and without the addition of zirconia powder were higher than 65% at 6 h after mixing. These values were much higher than that of the CPC paste without mechano-chemically modification, and similar to that of CPC with zirconia abrasion powder contamination. By contrast, the compression strength of the set CPC with zirconia powder additives were higher than that without the addition, and similar to that of CPC with zirconia abrasion powder contamination. These results suggest that the changes in the CPC powder properties due to mechano-chemically modification mainly affected the injectability of the CPC paste, and the zirconia abrasion powder contamination of the CPC powder affected the strength of the set CPC.

1. Introduction

Calcium phosphates in many different forms are of wide interest in the biomedical materials field because of their excellent biocompatibility, bioactivity, and osteoconductivity. In particular, calcium phosphate cements (CPCs) are promising as a minimally invasive bone substitute because they can be easily injected into bone defects, conforming to the shape of the defect and finally converting to natural bone based on their excellent osteoconductivity [1–4]. However, the strength of CPCs needs to be improved [5]. An effective process to increase the strength of CPCs after setting is increasing the powder-to-liquid (P/L) ratio for the CPC paste preparation. However, increases in the P/L ratio leads to a reduction in injectability. Therefore, to achieve excellent balance of high injectability and high strength of CPCs, another process is required. A promising process is the mechano-chemical improvement of CPC powder by reducing the powder size using ball-milling [6]. Mechano-chemically modified β-tricalcium phosphate (β-TCP) powder exhibited improved injectability of cement paste and strength of set cements (compact) [3,6]. Furthermore, the broader peaks of both β-TCP and zirconia were observed in the X-ray diffractometry (XRD) profiles of β-TCP powder after ball-milling [3]. The zirconia peaks indicated that zirconia abrasion powder from the milling pot and balls contaminated the β-TCP powder. Zirconia particles were reported to be effective in improving the compressive strength of the calcium phosphate cement compact [7]. Therefore, the strength increase in CPC using β-TCP powder after ball-milling partially depended on the property change in the β-TCP powder, and partially depended on the strengthening due to zirconia powder contamination. Moreover, it was reported that the

* Corresponding author. .
E-mail addresses: yennykim9106@gmail.com (Y. Kim), enchantee23@korea.kr (J. Bae), uyamanikofu@tokushima-u.ac.jp (E. Uyama), ksekine@tokushima-u.ac.jp (K. Sekine), fumiaki@tokushima-u.ac.jp (F. Kawano), hamada.dent@tokushima-u.ac.jp (K. Hamada).
[1] Present Address: Medical Device Safety Bureau, Ministry of Food and Drug Safety, 187 Osongsaengmyeong2-ro, Osong-eup, Heungdeok-gu, Cheongju-si, Chungcheongbuk-do, 28,159, Korea.

https://doi.org/10.1016/j.ceramint.2020.09.017
Received 3 July 2020; Received in revised form 26 August 2020; Accepted 1 September 2020
Available online 3 September 2020

addition of silica nanoparticles affected the injectability of CPC pastes [8], which suggests that the addition of zirconia particles also affects injectability.

The objective of this study is to evaluate separately the effect of property change in β-TCP powder and zirconia powder contamination on the strength of CPC compacts and injectability of CPC pastes. In this study, the authors found that changing the milling-ball material from magnesia-stabilized-zirconia (MgSZ) to yttria-stabilized-zirconia (YSZ) successfully reduced the zirconia contamination in β-TCP powder after ball-milling. CPC specimens in this study were prepared using ball-milled β-TCP powder with low zirconia contamination as a control, and two types of zirconia powders were used as additives: one was MgSZ powder extracted from ball-milled β-TCP powder with high zirconia contamination, and the other was nano size zirconia powder extracted from a commercial zirconia suspension. The control specimen was used to indicate the CPC properties that were mainly affected by the ball-milling process, while the specimens with additives were used to indicate the CPC properties that were affected by both ball-milling and zirconia powder contamination.

2. Materials and methods

2.1. Preparation of CPC

The same β-TCP powder (Taihei Chemical Industrial Co. Ltd., Osaka, Japan) used in a previous study was an ingredient of the CPC powder used in this study [3]. The β-TCP powder was modified using a planetary ball-mill (Pulverisette 7, Fritsch, Idar-Oberstein, Germany) and magnesia-stabilized-zirconia balls (15 mm diameter, Fritsch, Idar-Oberstein, Germany; MgSZ balls) or yttria-stabilized-zirconia balls (15 mm diameter, YTZ-15, Nikkato Co. Ltd., Osaka, Japan; YSZ balls). An amount of 8 g of the β-TCP powder, 4 mL of ethanol (99.5%), and 7 zirconia balls were placed in a zirconia pot (45 mL, Fritsch, Idar-Oberstein, Germany), and milled at a rotation speed of approximately 1000 rpm (motor speed), and the ball-milling time was set to 24 h. The powder was then dried in an oven at 60 °C for more than 12 h. The β-TCP powder before ball-milling was denoted cβ-TCP, and that after milling using each type of ball (MgSZ or YSZ) was denoted MgSZ-β-TCP and YSZ-β-TCP, respectively.

To clarify the effects of zirconia contamination in the CPC powder on the mechanical properties of CPC after setting, two types of zirconia powder additives were prepared. The first type is a zirconia abrasion powder extracted from the MgSZ-β-TCP powder. MgSZ-β-TCP powder was dissolved in a 3% hydrochloric acid solution, the residues were filtrated using filter paper (150 mm diameter, Whatman 1450–150, Cytiva, Sheffield, UK), and dried in an oven at 60 °C (extracted zirconia: eZR). The mass of both the MgSZ-β-TCP powder and the collected residues collected was measured and the ratio of zirconia contamination was calculated. YSZ-β-TCP powder was similarly dissolved and processed to calculate the ratio of zirconia contamination. The second type of additives is the zirconia powder of approximately 100 nm in diameter extracted from a commercial dispersion of 10 mass% zirconia in H_2O (643,025, Sigma-Aldrich, St. Louis, Missouri, USA). The dispersion was concentrated using centrifugation at a relative centrifugal force of 1000 *g* (R–300SII, Sakuma, Tokyo, Japan), and then dried in an oven at 60 °C to remove water (nano zirconia: nZR). The two types of additives were mixed into the YSZ-β-TCP powder at mixing ratios of *x* mass% and *y* mass% (*x*eZR-YSZ-β-TCP, *y*nZR-YSZ-β-TCP, where *x* and *y* indicates the mixing ratio of eZR and nZR; 1 mass%, 2 mass%, 3 mass%, 4 mass%, 5 mass%, and 6 mass%). After mixing the zirconia additives into the YSZ-β-TCP powder, the powder was mixed again using ball-milling for 24 h with YSZ balls.

To produce the two kinds of solutions, $CaCl_2$ (95.0%) and NaH_2PO_4 (99.0%) were mixed with distilled water according to their respective concentrations, and then filtrated using a PES Syringe Filter (0.45 μm pore size, 013045S-SFPES, AS ONE Corp., Osaka, Japan). The mixing ratio of prepared CPC powder to 1.0 M $CaCl_2$ solution to 0.6 M NaH_2PO_4 solution was 4:1:1 (g/mL/mL). The mixing time with the primary $CaCl_2$ solution was 5 min and that with the secondary NaH_2PO_4 solution was 1 min. The total powder to liquid (P/L) ratio and the Ca/P ratio of the mixing liquid was 2.0 (g/mL) and 1.67, respectively. Mixing of the powder and liquid was performed on a glass slab using a stainless-steel spatula, to prepare CPC paste.

2.2. Mechanical properties of compact

The compression strength (CS) and diametral tensile strength (DTS) of the CPC compact were evaluated. The CPC paste was filled into a silicone (KE-1300T, Shin-Etsu Chemical Co. Ltd., Tokyo, Japan) mold using a stainless-steel spatula. The specimens were then stored for setting in an incubator at 37 °C and a humidity of 100% for 1 week. The dimensions of the mold for the CS specimen were 3 mm in diameter and 6 mm in height, and those for the DTS specimen were 6 mm in diameter and 4 mm in height. The dimensions of the specimens were measured using a digital caliper. The CS and DTS of the specimens were evaluated using a universal testing machine (Autograph AGS-500A, Shimadzu Corp., Kyoto, Japan) at a crosshead speed of 10 mm/min. The number of the specimens was ten for both CS and DTS. The CS and DTS were calculated according to the following equations:

$$CS = \frac{F_{max}}{\pi \times d^2} \quad (1)$$

$$DTS = \frac{2 \times F_{max}}{\pi \times d \times l} \quad (2)$$

where d is the specimen diameter, F_{max} is the failure load, and l is the length of the specimen.

2.3. Characterization of β-TCP powder and specimen

The phase constitution of the CPC powder and compact after setting was identified using X-ray diffractometry (XRD; MiniFlex, Rigaku Corp., Tokyo, Japan) at a step size of 0.02°, using CuKα radiation at 30 kV and 15 mA. Data was collected in the 2θ range of 20–60° in a continuous mode with a scan speed of 0.1°/min. The XRD profiles were then analyzed using fityk software [9], and the lattice parameters were calculated.

The β-TCP powder before and after ball-milling, as well as the surface of the DTS specimen 1 week after mixing were gold-coated using an ion-coating apparatus (IB-3, Eiko Engineering Co. Ltd., Tokyo, Japan), and the morphology of the specimens was analyzed using scanning electron microscopy (SEM; JCM5700, JEOL Co. Ltd., Tokyo, Japan).

2.4. Particle size of powder

The particle size distribution of the CPC powder was evaluated using a centrifugal automatic particle analyzer (CAPA-300, Horiba Ltd., Kyoto, Japan). 5 mg of sample powder was suspended in 2.4 mL of isopropanol and then dispersed by applying ultrasonic pulsing for 5 min. Before every measurement, the viscosity and the density of isopropanol at room temperature (25 °C) were set to 1.96 cP and 0.78 g/cm^3, respectively. The density of the sample powders was determined as described in the following section (2.5).

2.5. Apparent porosity calculation

For the calculation of density and porosity of the compact, the DTS specimens were dehydrated at 50 °C in an oven for 1 day. The real volume (V_r) of the compact was measured using a gas pycnometer (AccuPyc 1330, Micromeritics Instrument, Norcross, GA, USA). The mass of the specimen (M) was measured using a microbalance. Triplicate measurements of volume and mass were conducted for each specimen,

and average values were employed. The apparent density (D_b), the solid density (D_s), and the porosity (P) of the compact were calculated using the following equations:

$$D_b = \frac{M}{\pi \times d^2 \times l} \quad (3)$$

$$D_s = \frac{M}{V_r} \quad (4)$$

$$P\ (\%) = (1 - \frac{D_b}{D_s}) \times 100 \quad (5)$$

2.6. Injectability

The injectability of the CPC paste is defined as the ability of a formulation to be extruded through a syringe fitted with a long needle [10]. For the measurement of injectability in this study, the following method was used. Approximately 2.8 g of the CPC paste was filled into a disposable syringe (2 mm inner-diameter opening, 12 mm inner-diameter body, and 10 mL inner volume (Terumo Syringe, Terumo Corp., Tokyo, Japan)) immediately after mixing. The syringe plunger was placed in contact with the paste fully into the syringe, and therefore, air retention was minimized inside the syringe. The six syringes were prepared and measured for up to 6 h, respectively. The CPC paste was extruded using a universal testing machine (Autograph AGS-500A, Shimadzu Corp., Kyoto, Japan) with a 1 kN load cell (Type SLBL-1kN, Shimadzu Corp., Kyoto, Japan) for the mechanical loading at a cross-head speed of 20 mm/min and a maximum force of 300 N. The maximum force of 300 N was selected as the typical maximum force exerted on a syringe plunger by hand [11]. The mass of the CPC paste in the syringes during mechanical loading was measured at 1 h intervals, and the mass of the CPC paste extruded from the syringe was calculated. The injectability was calculated using the following equation:

$$\text{Injectability}\ (\%) = \frac{W_{ext}}{W} \times 100 \quad (6)$$

where W_{ext} is the mass of the paste extruded from the syringe, and W is the initial mass of the paste in the syringe before injection.

2.7. Statistical analysis

All the data in this research was statistically analyzed using the Steel-Dwass Test in the EZR software [12], to compare the mean values from different groups. Statistical significance was accepted at a confidence level of 0.05.

3. Results

3.1. Effects of ball-milling on β-TCP powder

The XRD profiles of the β-TCP powder before and after ball-milling using each type of balls are shown in Fig. 1. A decrease in the crystallinity of β-TCPs with ball-milling was observed in which the XRD profile (after ball milling) partially resembled an amorphous phase. The calculated lattice parameters of cβ-TCP, MgSZ-β-TCP, and YSZ-β-TCP are shown in Table 1. Each parameter increased with ball-milling, and that of YSZ-β-TCP was larger than that of MgSZ-β-TCP.

The ratio of zirconia contamination extracted from MgSZ-β-TCP and YSZ-β-TCP was 6.2 mass% and 1.0 mass%, respectively. Additionally, in the profile of YSZ-β-TCP, weak zirconia peaks could be observed with β-TCP peaks. By contrast, in the profile of MgSZ-β-TCP, significant zirconia peaks could be observed with β-TCP peaks. These peaks indicated that the β-TCP powder contained zirconia contamination abraded from milling-pot and balls.

The SEM images of the β-TCP powder before and after ball-milling

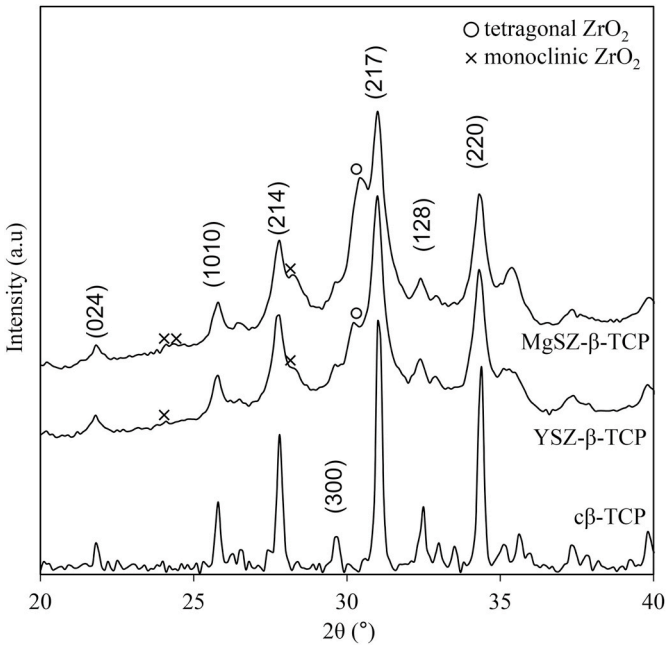

Fig. 1. XRD profiles of β-TCP powder without ball-milling (cβ-TCP) and β-TCP powder after ball-milling using each type of ball (MgSZ-β-TCP and YSZ-β-TCP).

Table 1
Cell parameters of cβ-TCP powder, MgSZ-β-TCP powder and YSZ-β-TCP powder.

Material	Lattice parameter		
	a,b (nm)	c (nm)	V (nm^3)
cβ-TCP	1.0430	3.7369	3.521
MgSZ-β-TCP	1.0440	3.7448	3.535
YSZ-β-TCP	1.0442	3.7508	3.542

are shown in Fig. 2. The cβ-TCP exhibited elliptical-shaped particles that were connected to each other. In contrast, the MgSZ-β-TCP and YSZ-β-TCP exhibited nano scale polygonal particles, which aggregated to form larger and reasonably spherical particles.

The XRD profiles of the zirconia powder extracted from a commercial dispersion (nZR) and that extracted from MgSZ-β-TCP powder (eZR) are shown in Fig. 3. The XRD profile of the nZR displayed peaks of cubic zirconia, tetragonal zirconia, and monoclinic zirconia, while the XRD profile of the eZR displayed peaks of tetragonal zirconia and monoclinic zirconia.

Fig. 4 shows the particle size distributions of the MgSZ-β-TCP powder, YSZ-β-TCP powder, 4eZR-YSZ-β-TCP powder, and 3nZR-YSZ-β-TCP powder. The particle size distributions of the extracted zirconia powder and nano zirconia powder are also indicated in Fig. 4.

3.2. Injectability of β-TCP cement paste

Fig. 5 shows the injectability of the MgSZ-β-TCP, YSZ-β-TCP, 2eZR-YSZ-β-TCP, and 1nZR-YSZ-β-TCP cement pastes. 2eZR-YSZ-β-TCP and 1nZR-YSZ-β-TCP indicated the highest CS in *x*eZR-YSZ-β-TCP and *y*nZR-YSZ-β-TCP, respectively. The calculated injectability at 6 h of the MgSZ-β-TCP cement paste and the YSZ-β-TCP cement paste after mixing was 88.3% and 79.7%, respectively. Furthermore, the calculated injectability at 6 h of the 2eZR-YSZ-β-TCP cement paste and 1nZR-YSZ-β-TCP cement paste after mixing was 66.6% and 69.7%, respectively.

3.3. Phase constitution of β-TCP cement compacts

The XRD profiles of the crushed cement compacts of MgSZ-β-TCP,

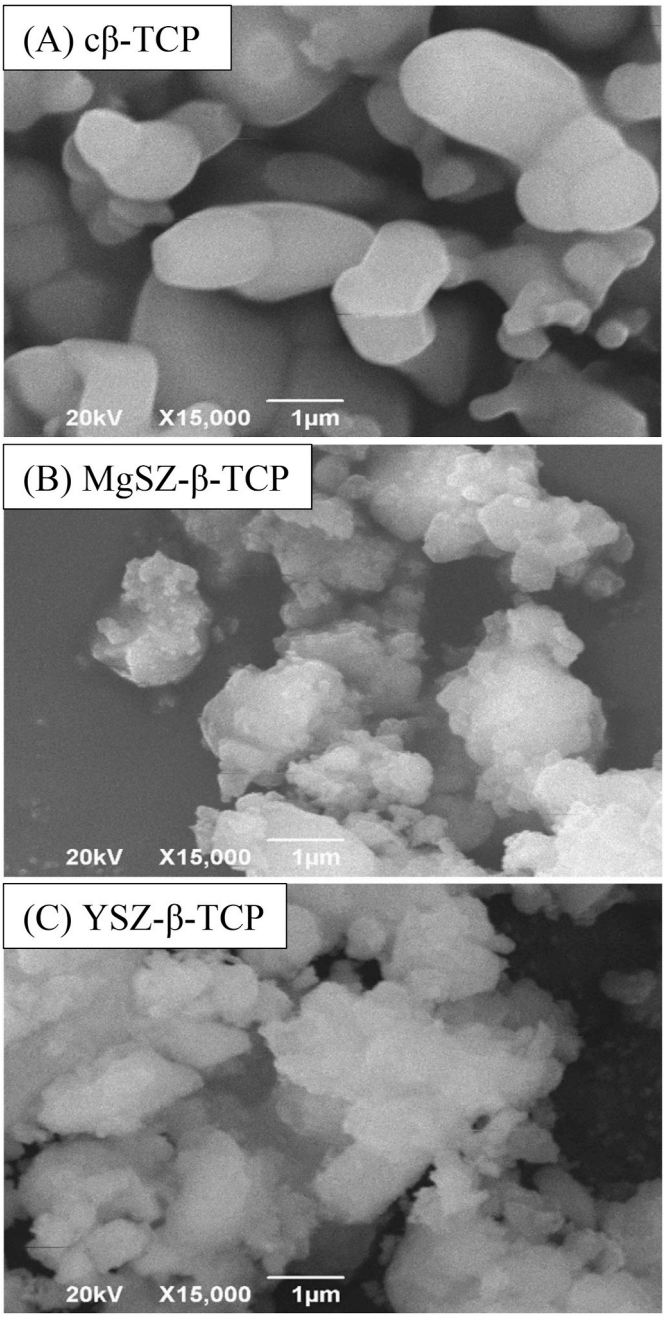

Fig. 2. SEM images of the β-TCP powder before and after ball-milling.

YSZ-β-TCP, 6eZR-YSZ-β-TCP, and 6nZR-YSZ-β-TCP after setting are shown in Fig. 6. In the patterns of all of the cement compacts, hydroxyapatite (HA) and zirconia peaks could be observed with weak β-TCP peaks. Note that, β-TCP peaks were hardly observed in the patterns of the set 6eZR-YSZ-β-TCP cement compact and the set 6nZR-YSZ-β-TCP cement compact.

3.4. Properties of β-TCP cement compacts

Fig. 7 shows the strength of the β-TCP cement specimens 1 week after mixing according to the types and content of zirconia additives. The DTS value of the eZR-YSZ-β-TCP compacts increased with zirconia content from a mixing ratio of 1%–4% and then decreased, and that of the nZR-YSZ-β-TCP compacts increased with zirconia content from a mixing ratio of 1%–3% and then decreased. The CS value of the eZR-YSZ-β-TCP compacts increased with zirconia content from a mixing ratio of 1%–2%

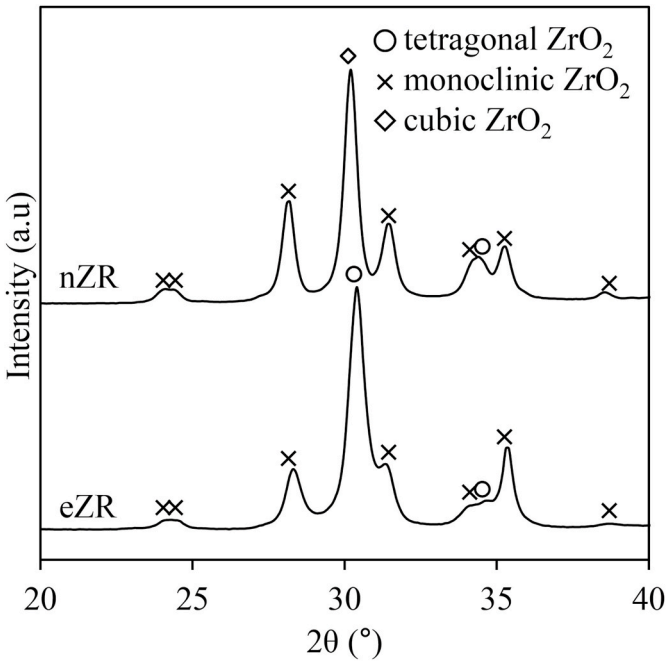

Fig. 3. X-ray diffraction profiles of two types of zirconia powder: nZR (extracted from a commercial zirconia dispersion) and eZR (extracted from MgSZ-β-TCP powder).

and then decreased, and that of the nZR-YSZ-β-TCP compacts showed a maximum value at a mixing ratio of 1% and then decreased.

Fig. 8 shows the CS and DTS values of the MgSZ-β-TCP compact and the YSZ-β-TCP compacts, and the highest CS values and DTS values of the YSZ-β-TCP cement compacts containing each zirconia additive. The CS value of the MgSZ-β-TCP cement compact and YSZ-β-TCP cement compact was 41.2 MPa and 22.6 MPa, respectively. The DTS value of the MgSZ-β-TCP cement compact and YSZ-β-TCP cement compact was 7.7 MPa and 4.9 MPa, respectively. The highest CS value of the eZR-YSZ-β-TCP cement was 34.7 MPa at 2eZR-YSZ-β-TCP, and that of the nZR-YSZ-β-TCP cement was 38.2 MPa at 1nZR-YSZ-β-TCP. The highest DTS values of the eZR-YSZ-β-TCP cement was 7.8 MPa at 4eZR-YSZ-β-TCP, and that of the nZR-YSZ-β-TCP cement was 7.5 MPa at 3nZR-YSZ-β-TCP.

Fig. 9 shows the correlation between CS and the porosity of the MgSZ-β-TCP cement compact, the YSZ-β-TCP cement compact, the 2eZR-YSZ-β-TCP cement compact indicating the highest CS value in the eZR-YSZ-β-TCP cement compacts, and the 1nZR-YSZ-β-TCP cement compact indicating the highest CS value in the nZR-YSZ-β-TCP compacts. The porosity values of the MgSZ-β-TCP cement compact and YSZ-β-TCP cement compact were 52% and 57%, respectively. The porosity values of the 2eZR-YSZ-β-TCP compact and the 1nZR-YSZ-β-TCP compact were 53% and 52%, respectively. The value of the YSZ-β-TCP compact was higher than the other values; however, all the porosity values were not significantly different.

3.5. SEM observation of cement compacts

The SEM-micrographs of the fracture surfaces of the DTS specimens 1 week after setting are shown in Fig. 10. The MgSZ-β-TCP specimen exhibited a rough agglomerated granular structure and the diameter of the grains was approximately 5 μm. By contrast, the fracture surface of the YSZ-β-TCP specimen contained many flat and smooth grains with diameters larger than approximately 10 μm, and numerous fine needle-like crystals were observed on the surface of the grains. A rough agglomerated granular structure was also observed on the fracture surface of the 4eZR-YSZ-β-TCP specimen and the 3nZR-YSZ-β-TCP specimen. The grain size of the 4eZR-YSZ-β-TCP specimen was similar to

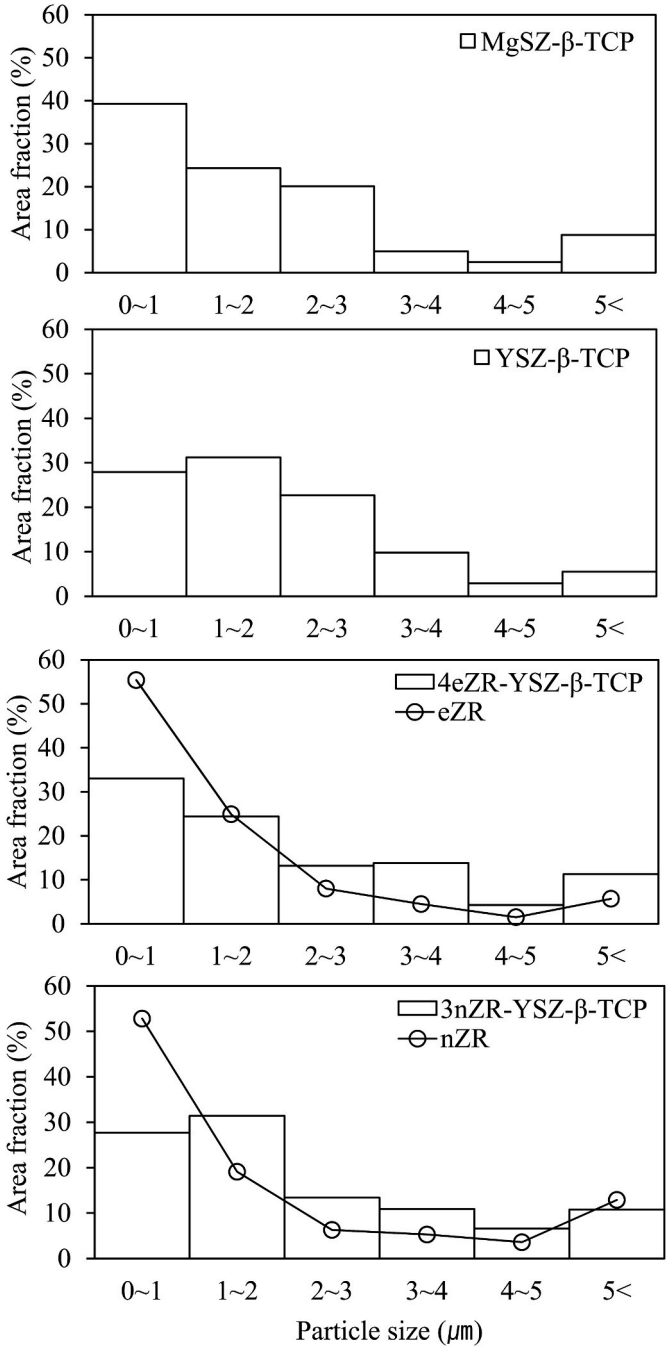

Fig. 4. Particle size distributions of the β-TCP powder after ball-milling using each type of balls and those containing the zirconia additives.

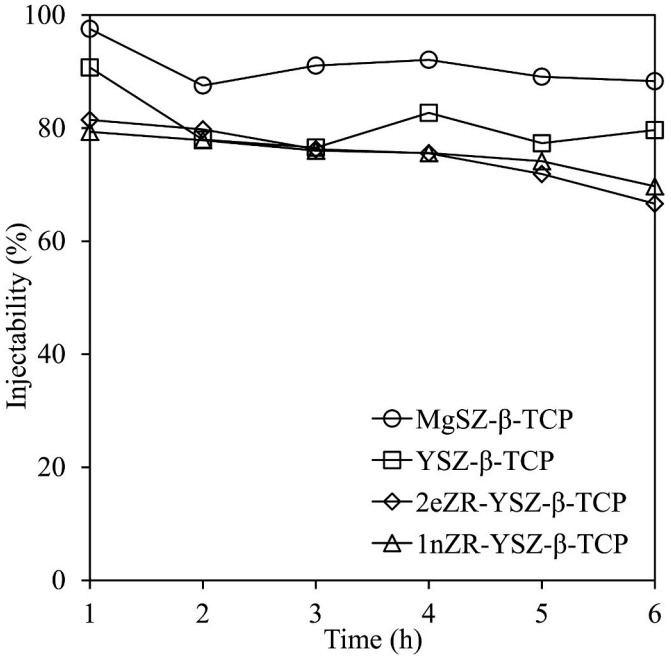

Fig. 5. Injectability of the MgSZ-β-TCP, YSZ-β-TCP, 2eZR-YSZ-β-TCP, and 1nZR-YSZ-β-TCP cement paste under a maximum force of 300 N.

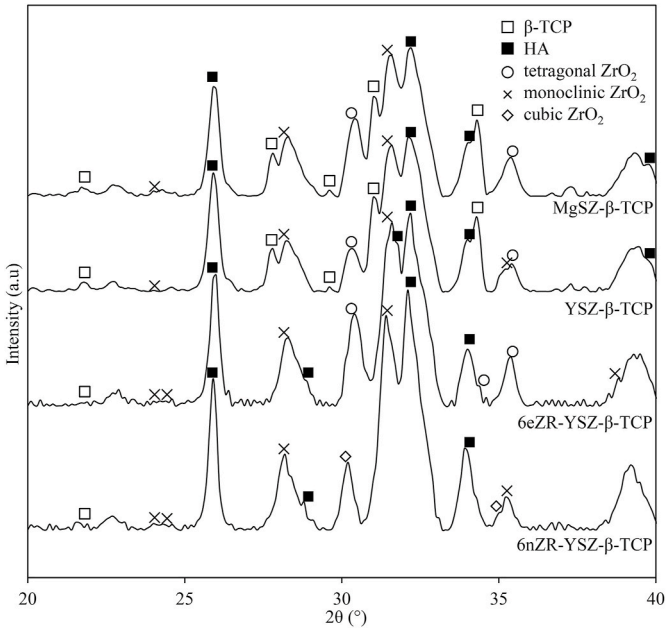

Fig. 6. XRD profiles of the crushed cement compact of MgSZ-β-TCP, YSZ-β-TCP, 6eZR-YSZ-β-TCP, and 6nZR-YSZ-β-TCP after setting.

that of the MgSZ-β-TCP specimen, while that of the 3nZR-YSZ-β-TCP specimen was larger than that of the MgSZ-β-TCP specimen and smaller than that of the YSZ-β-TCP specimen.

4. Discussion

4.1. Effects of ball-milling on CPC powder

A proportion of the zirconia contamination in the CPC powder after ball-milling was captured in the filter paper, and thus it was impossible to evaluate the precise mass of the zirconia contamination. Therefore, the remarkable difference in the ratio of the zirconia contamination extracted from the MgSZ-β-TCP powder and YSZ-β-TCP powder was considered. Although the mechanism of the difference in wear resistance of the zirconia balls in the present study was not clarified, the difference in the ratio of the zirconia contamination between the two powders suggested that the combination of the YSZ balls and MgSZ pot exhibited higher wear resistance. The difference in the zirconia contamination ratio is manifested in the weaker zirconia peaks in the XRD profile of the YSZ-β-TCP powder in Fig. 1, and in the difference between the XRD profiles of 6eZR-YSZ-β-TCP and that of MgSZ-β-TCP in Fig. 6. Therefore, the properties of the cement paste and the compact of YSZ-β-TCP with 6% eZR addition is not necessarily similar to those of MgSZ-β-TCP. The particles in the commercial zirconia dispersion might aggregate during

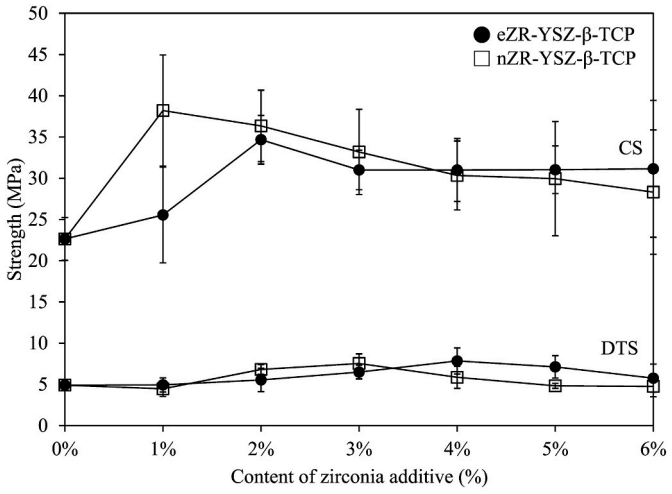

Fig. 7. Diametral tensile strength (DTS) and compression strength (CS) of the β-TCP cement compact 1 week after mixing.

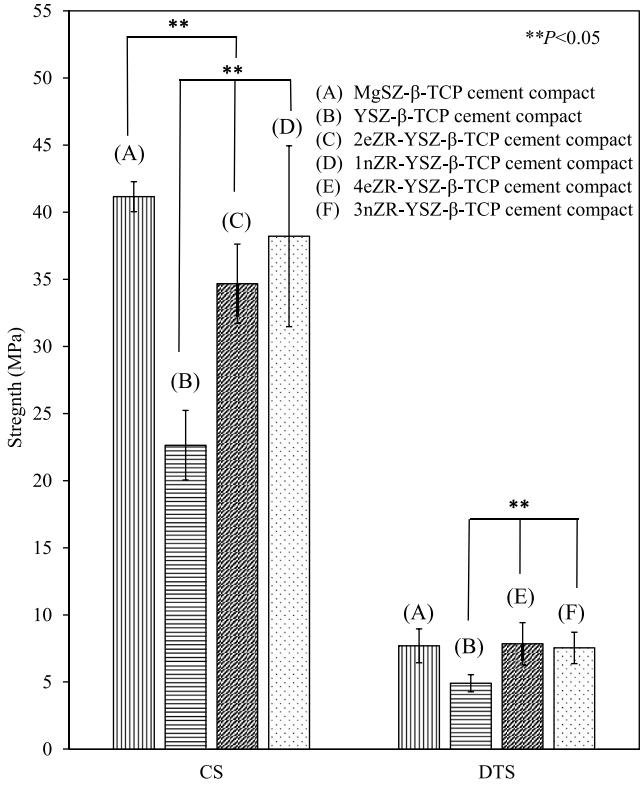

Fig. 8. CS and DTS values of the MgSZ-β-TCP cement compacts, and the highest CS and DTS values of the eZR-YSZ-β-TCP and nZR-YSZ-β-TCP cement compacts.

the particle separation process to form large particles, resulting in the high fraction of particles larger than 1 μm.

The particle size distributions of the β-TCP powder with zirconia contamination and β-TCP powder with zirconia powder additives in Fig. 4 are associated with the change in the particle size distribution after ball-milling. All the samples exhibited a relatively broad size distribution and more than half of the particles can be observed in the 0–2 μm range. Nevertheless, the addition of eZR and nZR did not induce a remarkable change in the particle size distribution of the CPC powder because of the relatively low amount of zirconia addition to the whole powder.

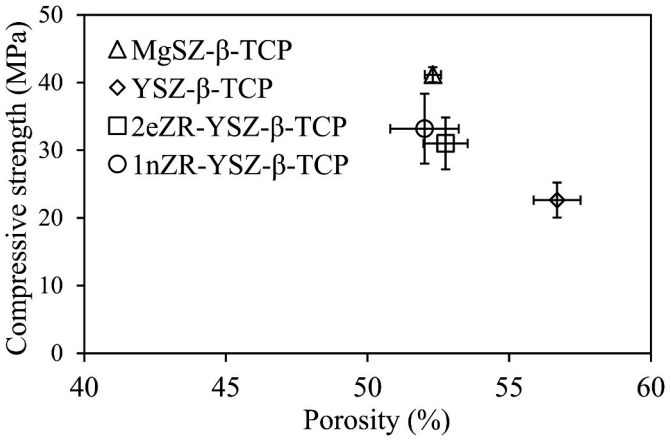

Fig. 9. Correlation between CS and the porosity of the MgSZ-β-TCP, YSZ-β-TCP, 2eZR-YSZ-β-TCP, and 1nZR-YSZ-β-TCP cement compacts.

Another effect of ball milling on the CPC powder was the change in crystallinity. The β-TCP powder modified by ball-milling induced a phase transformation from the crystalline phase to the amorphous phase, which leads to the formation of defects within the crystal lattice of β-TCP. The increase in the lattice parameters of the β-TCP powder after ball-milling supports defect formation within the lattice. The formation of defects reduces the crystal size, leading to a loss in crystallinity [6]. The reduced crystallinity of β-TCP could change its solubility, although it could not directly change the mechanical properties of the set cement compact because HA precipitated after the dissolution of the β-TCP particles.

4.2. Injectability of CPC paste

Our previous study indicated that the injectability of the β-TCP cement paste without ball-milling disappeared 60 min after mixing [3]. In contrast, β-TCP cement pastes after ball-milling, as shown in Fig. 5, exhibited excellent injectability (>65%) 6 h after mixing. The large difference between the cement with and without ball-milling suggested that cement powder modification using a ball-milling process remarkably affected the injectability. Note that the excellent injectability of YSZ-β-TCP cement with less zirconia contamination suggested that the zirconia contamination or additive was not part of the main mechanism for increasing the injectability. It is reported that small and spherical particles improve the fluidity of a powder-liquid mixture. This phenomenon is known as the ball-bearing effect [13]. In the present study, the spherical agglomerates in the cement paste after ball-milling potentially indicate that the ball-bearing effect increased the injectability. Moreover, MgSZ-β-TCP, 2eZR-YSZ-β-TCP, and 1nZR-YSZ-β-TCP in the present study also exhibited similar excellent injectability, suggesting that an appropriate level of zirconia contamination or additives resulted in neutral or positive effects on injectability. The contributions of zirconia particles to the injectability improvement were reported to be the round shape of deagglomerated particles and a broad particle size distribution [14]. However, the present study indicated that the addition of 2eZR and 1nZR in the cement powder was less effective in improving the injectability of the cement paste. Moreover, premixed CPC containing zirconia powder was reported to extend the setting time and reduce the compressive strength [15]. Therefore, the optimization of the zirconia content in the cement paste should be considered from several viewpoints.

4.3. Phase constitution of CPC compacts

Fig. 6 shows that significant HA and zirconia peaks were observed in the profiles of all the cement compacts. Interestingly, the β-TCP peaks

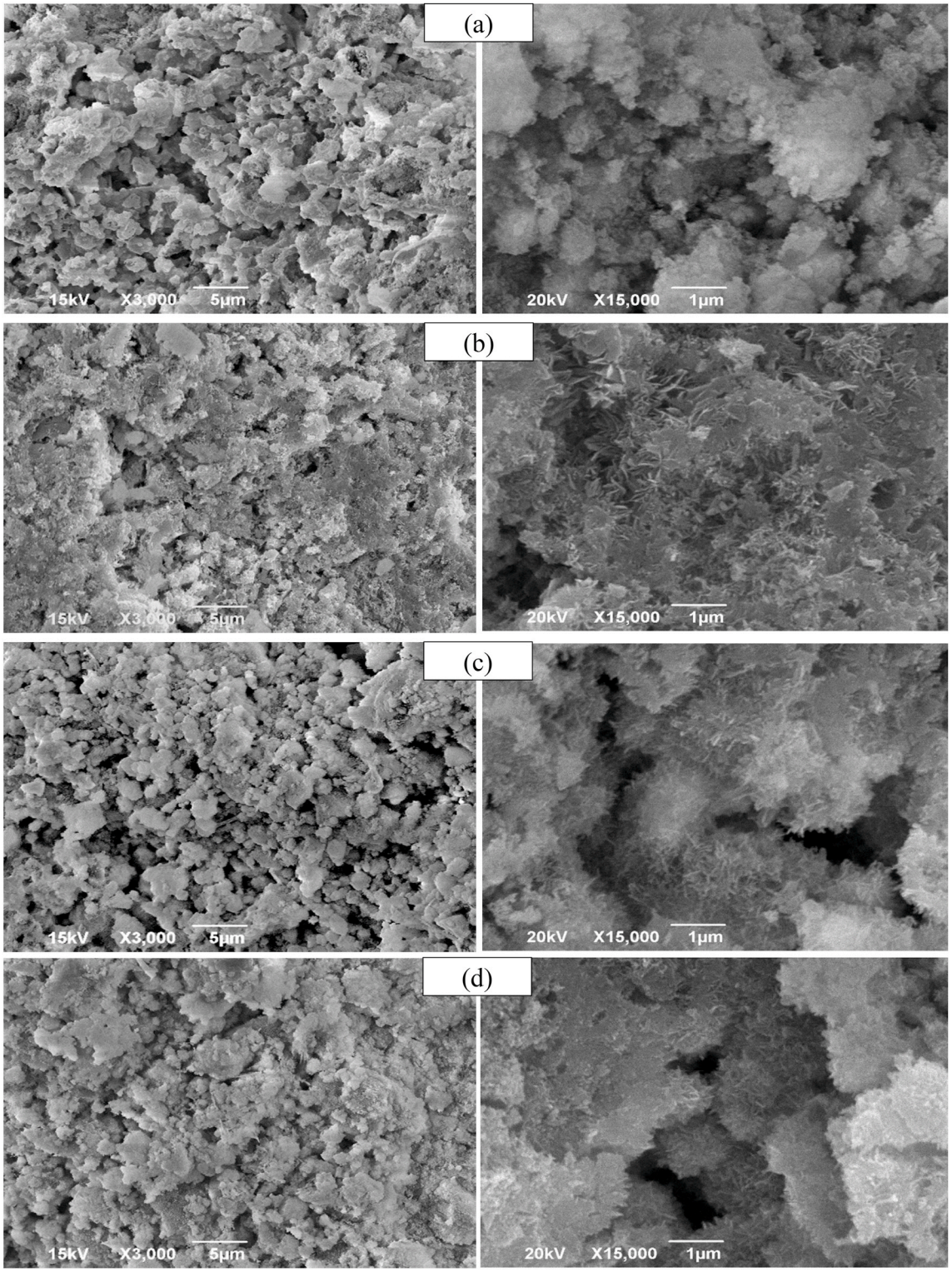

Fig. 10. SEM images of the fracture surfaces of the DTS specimens 1 week after setting. (a) MgSZ-β-TCP cement compact, (b) YSZ-β-TCP cement compact, (c) 4eZR-YSZ-β-TCP cement compact, (d) 3nZR-YSZ-β-TCP cement compact.

were hardly observed in the profiles of the set 6eZR-YSZ-β-TCP cement compact and the set 6nZR-YSZ-β-TCP cement compacts, suggesting that the addition of eZR particles and nZR particles accelerated the dissolution of β-TCP. However, it is difficult for solid phase zirconia to affect the dissolution of β-TCP into water. Therefore, a more plausible mechanism for the disappearance of β-TCP is as follows. Zirconia particles, acting as precipitation nuclei, accelerated the precipitation of HA, thereby reducing the concentration of calcium and phosphate ions in the solution of cement paste, and thus facilitating β-TCP dissolution.

4.4. Properties of CPC compacts

Fig. 7 shows that with increasing zirconia additive ratio, the strength of both eZR-YSZ-β-TCP and nZR-YSZ-β-TCP increased, and then

decreased. Notably, all the CS values of both eZR-YSZ-β-TCP and nZR-YSZ-β-TCP were significantly higher than that of YSZ-β-TCP (equal to 0eZR-YSZ-β-TCP and 0nZR-YSZ-β-TCP) except for 1eZR-YSZ-β-TCP, 6eZR-YSZ-β-TCP, and 6nZR-YSZ-β-TCP. The maximum DTS values of both eZR-YSZ-β-TCP and nZR-YSZ-β-TCP were significantly higher than that of YSZ-β-TCP and were similar to that of MgSZ-β-TCP, as observed in Fig. 8. The zirconia particles accelerating the growth of HA precipitation network is likely the cause of the increased strength of the cement compact in the present study.

Fig. 8 shows that the MgSZ-β-TCP specimen exhibited the highest strength, while the YSZ-β-TCP specimen exhibited significantly lower CS and DTS values. Although the Ca/P ratio of the MgSZ-β-TCP and YSZ-β-TCP cements is the same and the crystallinity of HA observed in XRD profiles also appear similar, there are significant differences in the strength and potential amount of zirconia contamination. These results suggest that the differences between the properties of the two cements was mainly due to the potential amount of zirconia contamination. In other words, the property changes from the cement without ball-milling to YSZ-β-TCP mainly depended on the ball-milling effect, and the additional property change from YSZ-β-TCP to MgSZ-β-TCP mainly depended on the zirconia contamination effect. The hydroxyl groups on the zirconia surface combine with calcium ions to promote the formation of HA [16]. This combination could enhance the bonding between the calcium on the cement matrix surface and the hydroxyl groups on the zirconia surface, resulting in potential improvement of strength of the cement matrix [7]. On the contrary, zirconia additives were reported to reduce the compressive strength of the cement in a separate study [15]; the mechanism of this “opposite” effect of the zirconia additives is difficult to clarify. However, one potential mechanism might be due to the dry heat sterilization of the cement powder at 200 °C. The process could remove the hydroxyl groups on the zirconia surface, resulting in a loss of interaction between the zirconia surface and HA. In the present study, the cement powder was ball-milled in ethanol which is known as a dehydrating agent. Therefore, this process might also reduce the interaction between the zirconia surface and HA. However, the strengthening effect of the zirconia additives in the present study suggests that the cement powder preparation process in the present study is effective in improving the strength of CPC.

Fig. 9 shows that a reduced porosity increased the strength of the cement compacts, suggesting that a low porosity of the cement compacts containing a higher zirconia content supported a higher strength than that of the YSZ-β-TCP cement compact. Note that although the porosity of the MgSZ-β-TCP cement compacts was similar to those of the cement compacts containing zirconia additives, the strength of the former was higher than those of the latter. This difference suggests that not only the porosity but also the pore size distribution and/or pore shape affects the strength of the cement compact. However, the effects of the latter two properties were not investigated in the present study.

4.5. SEM observation of CPC compact

HA bone cements reinforced with zirconia particles were reported to exhibit a surface structure consisting of clusters with needle-like and plate-like crystals [5]. Similarly, a highly developed needle-like, plate-like, or grain-like HA crystal network was observed on the fracture surface of each CPC specimen in this study. Note that a rough agglomerated granular structure was observed only on the surface of the CPC specimens containing a higher zirconia contamination or additive content, and many flat and smooth grains were observed only on the surface of the YSZ-β-TCP specimen containing a lower zirconia contaminant content. This difference in the fracture surface morphology seems to be consistent with the difference in strength; a spherical fracture surface is generally the result of ductile fracture while a flat fracture surface is generally the result of brittle fracture, and brittle ceramic materials usually exhibit lower strength. The cause of the different macroscopic surface morphology is not clarified in the present study. However, a smaller zirconia content potentially caused the difference, because the smaller zirconia content in CPC indicates an overall smaller hydroxyl group content, resulting in less interactions that enhances the bonding between the calcium on the cement matrix surface and the hydroxyl groups of the zirconia surface. Since the interactions actually form between many crystals, less interactions leads to less growth of the HA crystal network. This mechanism might concomitantly increase the porosity and/or pore size. However, the fracture surfaces observed in the present study did not reveal a difference in the crystal network growth.

5. Conclusions

In the present study, the individual effect of ball-milling and zirconia powder contamination on the properties of the β-TCP cement paste and compact was investigated and the results are summarized as follows:

1. The injectability of the β-TCP cement paste was improved mainly due to the mechano-chemical modification using ball-milling, and not due to the zirconia contamination. The improvement was potentially caused by changes in the particle shape to spherical, and broadening of the particle size distribution.
2. The strength of the β-TCP cement compact was improved due to both the mechano-chemical modification using ball-milling and the zirconia contamination. The improvement was caused by the low porosity, and additionally, by the excellent development of HA crystal networks.
3. Appropriate addition of zirconia particles to the β-TCP cement powder containing less zirconia contamination is effective in improving the strength of the cement compact. As less contamination of zirconia means less weight loss of milling balls and jar, this low contamination ball-milling process has the advantage of extending the lifetime of the milling balls and jar, thus reducing the cost of processing. Although the cost of commercial dispersions of zirconia is not low, a long lifetime of the ball-milling equipment enables a constant mechano-chemical modification and a constant production of the modified β-TCP cement powder.

Declaration of competing interest

The authors declare that they have no known competing financial interests or personal relationships that could have appeared to influence the work reported in this paper.

Acknowledgements

This study was partially supported by the Japan Society for the Promotion of Science (JSPS, KAKENHI Grant numbers 16K20504 and 16K11626).

References

[1] D.S.H. Lee, Y. Pai, S. Chang, Effect of thermal treatment of the hydroxyapatite powders on the micropore and microstructure of porous biphasic calcium phosphate composite granules, J. Biomaterials Nanobiotechnol. 4 (2013) 114–118, https://doi.org/10.4236/jbnb.2013.42015.

[2] J. Zhang, W. Liu, V. Schnitzler, F. Tancret, J.-M. Bouler, Calcium phosphate cements for bone substitution: chemistry, handling and mechanical properties, Acta Biomater. 10 (2014) 1035–1049, https://doi.org/10.1016/j.actbio.2013.11.001.

[3] J. Bae, Y. Ida, K. Sekine, F. Kawano, K. Hamada, Effects of high-energy ball-milling on injectability and strength of β-tricalcium-phosphate cement, J. Mech. Behav. Biomed. Mater. 47 (2015), https://doi.org/10.1016/j.jmbbm.2015.03.005.

[4] A. Bigi, B. Bracci, S. Panzavolta, Effect of added gelatin on the properties of calcium phosphate cement, Biomaterials 25 (2004) 2893–2899.

[5] W. Yu, X. Wang, J. Zhao, Q. Tang, M. Wang, X. Ning, Preparation and mechanical properties of reinforced hydroxyapatite bone cement with nano-ZrO 2, Ceram. Int. 41 (2015) 10600–10606, https://doi.org/10.1016/j.ceramint.2015.04.159.

[6] U. Gbureck, O. Grolms, J.E. Barralet, L.M. Grover, R. Thull, Mechanical activation and cement formation of β -tricalcium phosphate, Biomaterials 24 (2003) 4123–4131, https://doi.org/10.1016/S0142-9612(03)00283-7.
[7] K. Takahashi, Y. Fujishiro, S. Yin, T. Sato, Preparation and compressive strength of α-tricalcium phosphate based cement dispersed with ceramic particles, Ceram. Int. 30 (2004) 199–203, https://doi.org/10.1016/S0272-8842(03)00089-0.
[8] L.S. Mendes, S. Saska, F. Coelho, T.S.D.O. Capote, R.M. Scarel-Caminaga, R. Marchetto, R.G. Carrodeguas, A.M.M. Gaspar, M.A. Rodríguez, Injectable β-TCP/MCPM cement associated with mesoporous silica for bone regeneration: Characterization and toxicity evaluation, Biomed. Mater. 13 (2018), https://doi.org/10.1088/1748-605X/aa9085.
[9] M. Wojdyr, Fityk: A general-purpose peak fitting program, J. Appl. Crystallogr. 43 (2010) 1126–1128, https://doi.org/10.1107/S0021889810030499.
[10] S. V Dorozhkin, Self-setting calcium orthophosphate formulations, J. Funct. Biomater. 4 (2013) 209–311, https://doi.org/10.3390/jfb4040209.
[11] Y.B. Kim, B.M. Lee, M.C. Lee, I. Noh, S.-J. Lee, S.S. Kim, Preparation and characterization of calcium phosphate cement of α-tricalcium phosphate-tetracalcium phosphate-dicalcium phosphate system incorporated with poly (γ-glutamic acid), Macromol. Res. 21 (2013) 892–898.
[12] Y. Kanda, Investigation of the freely available easy-to-use software 'EZR' for medical statistics, Bone Marrow Transplant. 48 (2013) 452–458.
[13] L.G. Baltazar, F.M.A. Henriques, M.T. Cidade, Rheology of natural hydraulic lime grouts for conservation of stone masonry—influence of compositional and processing parameters, Fluid 4 (2019), https://doi.org/10.3390/fluids4010013.
[14] M. Bohner, G. Baroud, Injectability of calcium phosphate pastes, Biomaterials 26 (2005) 1553–1563, https://doi.org/10.1016/j.biomaterials.2004.05.010.
[15] J. Åberg, E. Pankotai, G. Hulsart Billström, M. Weszl, S. Larsson, C. Forster-Horváth, Z. Lacza, H. Engqvist, Vivo evaluation of an injectable premixed radiopaque calcium phosphate cement, Int. J. Biomater. (2011) 7, https://doi.org/10.1155/2011/232574, 2011.
[16] M.M. Pereira, A.E. Clark, L.L. Hench, Effect of texture on the rate of hydroxyapatite formation on gel-silica surface, J. Am. Ceram. Soc. 78 (9) (1995) 2463–2468, https://doi.org/10.1111/j.1151-2916.1995.tb08686.x.

ABBREVIATIONS

β–TCP: β–tricalcium phosphate, CPC: calcium phosphate cement, HA: Hydroxyapatite, MgSZ: magnesia-stabilized-zirconia, YSZ: yttria-stabilized-zirconia, SEM: scanning electron microscopy